

ψ production in $\bar{p}N$ and π^-N interactions at 125 GeV/c and a determination of the gluon structure functions of the \bar{p} and the π^-

C. Akerlof,⁴ H. Areti,^{3,*} M. Binkley,² S. Conetti,^{3,†} B. Cox,^{2,†} J. Enagonio,²
 He Mao,⁵ C. Hojvat,² D. Judd,^{2,‡} S. Katsanevas,¹ R. D. Kephart,² C. Kourkoumelis,¹ P. Kraushaar,^{4,§}
 P. Lebrun,^{3,*} P. K. Malhotra,^{2,||} A. Markou,¹ P. O. Mazur,² D. Nitz,⁴ L. K. Resvanis,¹ D. Ryan,³
 T. Ryan,^{3,¶} W. Schappert,^{3,**} D. G. Stairs,³ R. Thun,⁴ F. Turkot,² S. Tzamarias,^{1,††} G. Voulgaris,¹
 R. L. Wagner,² D. E. Wagoner,^{2,‡} W. Yang,² and Zhang Nai-jian⁵

(E537 Collaboration)

¹University of Athens, Athens, Greece

²Fermi National Accelerator Laboratory, Batavia, Illinois 60510

³McGill University, Montreal, Quebec, Canada H3A 2T8

⁴University of Michigan, Ann Arbor, Michigan 48109

⁵Shandong University, Jinan, People's Republic of China

(Received 9 February 1993)

We have measured the cross section for production of ψ and ψ' in \bar{p} and π^- interactions with Be, Cu, and W targets in experiment E537 at Fermilab. The measurements were performed at 125 GeV/c using a forward dimuon spectrometer in a closed geometry configuration. The gluon structure functions of the \bar{p} and π^- have been extracted from the measured $d\sigma/dx_F$ spectra of the produced ψ 's. From the $\bar{p}W$ data we obtain, for \bar{p} , $xG(x) = (2.15 \pm 0.7)[1-x]^{(6.83 \pm 0.5)} [1 + (5.85 \pm 0.95)x]$. In the π^- case, we obtain, from the W and the Be data separately, $xG(x) = (1.49 \pm 0.03)[1-x]^{(1.98 \pm 0.06)}$ (for π^-W), $xG(x) = (1.10 \pm 0.10)[1-x]^{(1.20 \pm 0.20)}$ (for π^-Be).

PACS number(s): 13.85.Ni, 12.38.Qk, 14.40.Gx

I. INTRODUCTION

A large fraction of the ψ hadroproduction cross section is thought to be due to "fusion" between projectile and target gluons [1]. ψ hadroproduction can, therefore, be used to determine the gluon structure functions of the target nucleon and beam hadron. We have measured ψ production in a hadron beam from beryllium, copper, and tungsten targets and have extracted the projectile gluon distributions.

To determine accurately the gluon structure functions knowledge of the quark structure functions of the interacting hadrons is required, since some fraction of the production of ψ and ψ' is due to quark interactions. The

quark structure functions of the nucleons have been independently measured in deep-inelastic-scattering experiments [2]. The pion quark structure functions have been determined through the study of Drell-Yan production of high-mass muon pairs. As large- A nuclei are involved, the modified wave functions of quarks and gluons inside a heavy nucleus must be considered [3,4]. We have extracted the gluon structure functions independently for each target nucleus.

In Fermilab experiment E537 [5], we have measured the production of ψ , ψ' , and the Drell-Yan dimuon continuum by interactions of antiprotons and pions with Be, Cu, and W targets at 125 GeV/c. We have determined the quark structure functions for both \bar{p} and π^- from the Drell-Yan measurements [6]. Use of quark structure functions determined from the high-mass muon pair continuum in the same experiment as the measurement of ψ and ψ' production minimizes the systematic errors in the determination of the gluon structure functions.

II. THE SPECTROMETER

The measurement of the production of high-mass dimuons in experiment E537 has been performed using a tertiary 125 GeV/c \bar{p} and π^- beam in the High Intensity Laboratory at Fermilab. The enriched antiproton beam produced by Λ^0 , $\bar{\Lambda}^0$, and K_S^0 decays contained 18% \bar{p} and 82% π^- .

The large aperture spectrometer, described in detail elsewhere [5], is shown in Fig. 1. The apparatus included

*Present address: Fermilab, Batavia, Illinois 60510.

†Present address: University of Virginia, Charlottesville, Virginia 22903.

‡Present address: Prairie View A&M University, Prairie View, Texas 77445.

§Present address: Shell Oil, Houston, Texas.

||Deceased (permanent address was Tata Institute, Bombay, India).

¶Present address: Cornell University, Ithaca, New York 14853-2501.

**Present address: University of Chicago, Chicago, Illinois 60637.

††Present address: CERN, Geneva, Switzerland.

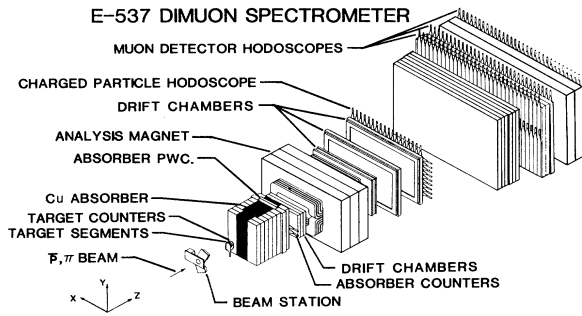


FIG. 1. The E537 spectrometer.

Be, Cu, and W targets, a Cu hadron absorber, a large aperture dipole analysis magnet, 20 proportional and drift multiwire chamber planes used as tracking elements, scintillation counter hodoscopes, and muon detector consisting of three planes of scintillation counters embedded in 300 tons of steel and concrete.

The first level fast dimuon trigger required at least two threefold coincidences among aligned counters in each of the three muon hodoscope planes, at least two hits in the charged particle hodoscope, and a \bar{p} or π^- signal from the beam tagging system. Events which satisfied the fast trigger were then sent to a dedicated second level ECL-CAMAC trigger processor [7] which kept only candidates with an effective mass greater than $2.0 \text{ GeV}/c^2$.

III. THE DATA SAMPLE

The total data sample accumulated using the W target contained 12 530 ψ events produced by the \bar{p} beam and 33 820 ψ events by the π^- beam. Figures 2(a) and 2(b) show the effective-mass distributions of the muon pairs. Fits of Gaussian forms to the ψ and ψ' peaks plus an exponential function of the $\mu^+\mu^-$ continuum are shown superimposed on the data. In addition, 529 ψ events from \bar{p} Cu, 1958 from π^- Cu, 588 from \bar{p} Be, and 2881 from π^-

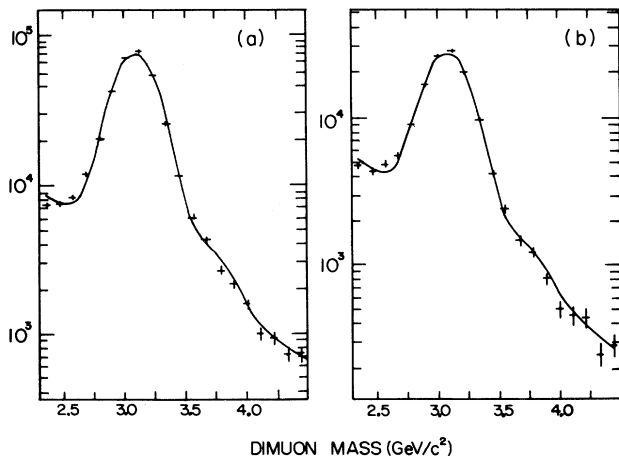


FIG. 2. (a) $\mu^+\mu^-$ invariant mass for $125 \text{ GeV}/c$ π^- W interactions. (b) $\mu^+\mu^-$ invariant mass for $125 \text{ GeV}/c$ \bar{p} W interactions.

Be interactions were collected. The mass resolution ($\sigma = 180 \text{ MeV}/c^2$ for the W target, $\sigma = 140 \text{ MeV}/c^2$ for the Cu target, and $\sigma = 200 \text{ MeV}/c^2$ for the Be target) was dominated by the target length and by the multiple scattering in the target and the Cu absorber.

Monte Carlo simulations have been used to correct the data for geometric acceptances, hardware inefficiencies, reinteractions in the target, trigger processor inefficiency, vertex cut inefficiency, accidental coincidences, and reconstruction inefficiencies [6]. The dependence of the cross section on the kinematical variables x_F , p_t , $\cos\theta$, and ϕ have been extracted from the corrected data using a maximum likelihood technique [6(b)].

IV. DIFFERENTIAL AND TOTAL CROSS SECTIONS

In a previous publication we have reported our measurement of the ψ production cross section in \bar{p} and π^- interactions with Be, Cu, and W targets [4]. Using the observed A dependence of the π^- data together with the H_2 and Pt results of Na3 [8], the total cross section per nucleon at $125 \text{ GeV}/c$ has been determined to be

$$\sigma(\bar{p}N \rightarrow \psi + X) = 52.59 \pm 1.7 \pm 3.15 \text{ nb/nucleon}$$

and

$$\sigma(\pi^- N \rightarrow \psi + X) = 63.06 \pm 2.0 \pm 3.78 \text{ nb/nucleon}.$$

The first error is due to the statistical uncertainty of the parametrization, and the second error is due to the systematic uncertainty in the beam flux normalization.

The ratio of ψ' to ψ production for \bar{p} 's and π^- 's has been determined from our high statistics W target data. The observed ratios of the number of ψ and ψ' decaying into $\mu^+\mu^-$ are

$$\frac{\psi' \rightarrow \mu^+\mu^-}{\psi \rightarrow \mu^+\mu^-} = 2.0 \pm 1.0 \% \quad \text{and} \quad 2.6 \pm 0.7 \%$$

for \bar{p} W and π^- W, respectively. Correcting for the muon pair branching ratios of ψ and ψ' we find

$$\frac{\sigma(\psi')}{\sigma(\psi)} = 18.50 \pm 9.25 \% \quad \text{for } \bar{p}\text{W interactions,}$$

$$\frac{\sigma(\psi')}{\sigma(\psi)} = 24.05 \pm 6.50 \% \quad \text{for } \pi^- \text{W interactions.}$$

Using the ψ' inclusive cross section derived from these ratios and the measured branching ratio for the $\psi' \rightarrow \psi + X$ decay [9], we find the fraction of the observed ψ coming from ψ' decay to be $9.8 \pm 4.5 \%$ and $12.7 \pm 3.5 \%$ for \bar{p} W and π^- W interactions, respectively. This is consistent with the WA11 [10] measurement of 8% in π^- Be interactions at $190 \text{ GeV}/c$.

The differential cross sections $d\sigma/dx_F$, $d\sigma/dp_{t,2}$, $d\sigma/d\cos\theta$, and $d\sigma/d\phi$ (where θ and ϕ are the Gottfried-Jackson decay angles) for ψ production in π^- N interactions are presented in Tables I (a)–(c) and in \bar{p} interactions in Tables II (a)–(c).

The differential cross sections per nucleon have been obtained by scaling the measured value, per nucleus, by a constant factor independent of x_F and p_t . This factor is

TABLE I. (Continued).

p_t^2 (GeV/c ²)	$d\sigma/dp_t^2$		x_F	$d\sigma/dx_F$	
	[nb/(GeV/c) ²] per Cu nucleus	[nb/(GeV/c) ²] per nucleon		(nb/Be nucleus)	(nb/nucleon)
2.250	478±34	8.36±0.60	0.750	180±133	20.3±15.0
3.150	206±22	3.60±0.38	0.850	116±158	13.1±17.9
4.050	117±16	2.06±0.29	0.950	0±131	0.0±14.8
4.950	62±12	1.09±0.20			
5.850	45±10	0.79±0.18			
6.750	12±5	0.22±0.09			
7.650	12±5	0.21±0.09			
8.550	14±7	0.24±0.11			
$\cos\theta$	$d\sigma/d\cos\theta$		p_t^2 (GeV/c ²)	$d\sigma/dp_t^2$	
	(nb/Cu nucleus)	(nb/nucleon)		[nb/(GeV/c) ²] per Be nucleus	[nb/(GeV/c) ²] per nucleon
-0.90	1 302±280	22.8±4.9	0.450	332±11	37.44±1.19
-0.70	1 646±162	28.8±2.8	1.350	120±6	13.49±0.70
-0.50	1 516±119	26.5±2.1	2.250	61±4	6.87±0.50
-0.30	1 696±114	29.7±2.0	3.150	28±3	3.11±0.33
-0.10	1 692±109	29.6±1.9	4.050	14±2	1.57±0.23
0.10	1 839±114	32.2±2.0	4.950	10±2	1.17±0.21
0.30	1 587±109	27.8±1.9	5.850	5±1	0.57±0.14
0.50	1 658±128	29.0±2.2	6.750	5±1	0.58±0.14
0.70	1 901±185	33.3±3.2	7.650	2±1	0.18±0.09
0.90	2 048±375	35.8±6.6	8.550	1±1	0.08±0.08
ϕ (deg)	$d\sigma/d\phi$		$\cos\theta$	$d\sigma/d\cos\theta$	
	(nb/Cu nucleus)	(nb/nucleon)		(nb/Be nucleus)	(nb/nucleon)
18.0	10.1±0.86	0.176±0.015	-0.90	226±44	25.5±5.0
54.0	9.6±0.75	0.168±0.013	-0.70	260±24	29.3±2.7
90.0	8.7±0.66	0.152±0.011	-0.50	232±17	26.1±1.9
126.0	10.1±0.76	0.177±0.013	-0.30	270±16	30.5±1.8
162.0	10.3±0.86	0.180±0.015	-0.10	254±15	28.7±1.7
198.0	9.4±0.82	0.165±0.014	0.10	270±16	30.5±1.8
234.0	9.6±0.75	0.167±0.013	0.30	286±17	32.2±1.9
270.0	9.6±0.68	0.167±0.012	0.50	257±19	28.9±2.1
306.0	8.3±0.69	0.146±0.012	0.70	242±23	27.3±2.6
342.0	9.2±0.83	0.161±0.014	0.90	175±35	19.7±3.9
x_F	$d\sigma/dx_F$		ϕ (deg)	$d\sigma/d\phi$	
	(nb/Be nucleus)	(nb/nucleon)		(nb/Be nucleus)	(nb/nucleon)
0.050	1 030±67	116.2±7.5	18.0	1.5±0.12	0.173±0.014
0.150	1 049±51	118.3±5.7	54.0	1.4±0.11	0.159±0.012
0.250	912±42	102.9±4.7	90.0	1.4±0.10	0.159±0.011
0.350	861±44	97.1±5.0	126.0	1.3±0.10	0.151±0.011
0.450	642±46	72.5±5.1	162.0	1.4±0.12	0.158±0.013
0.550	442±53	49.9±6.0	198.0	1.6±0.12	0.180±0.014
0.650	333±74	37.5±8.4	234.0	1.4±0.10	0.157±0.011
			270.0	1.5±0.10	0.174±0.011
			306.0	1.3±0.10	0.148±0.011
			342.0	1.6±0.12	0.175±0.014

the ratio between the measured total ψ production cross section for a given beam and nucleus and the extrapolation for $A = 1$ quoted above for that beam [4].

The errors quoted in the π^- differential cross sections per nucleon do not include a 3, 4, and 4.5 % error due to the A -dependence extrapolation for the π^-W , π^-Cu , and π^-Be data, respectively. Similarly a 3.5, 5, and 5 % error in the $\bar{p}W$, $\bar{p}Cu$, and $\bar{p}Be$ data is not included in the antiproton differential cross sections per nucleon.

V. COMPARISON OF THE \bar{p} DATA TO THE SEMILOCAL DUALITY MODEL

For the purpose of extracting the gluon extraction function we have used the semilocal duality model (SLDM) [11] which contains quark-antiquark and gluon-gluon fusion contributions to charmonium production. We have assumed that the SLDM describes the production of all the charmonium states. The prediction of the SLDM is

TABLE II. (Continued).

p_t^2 (GeV/c) ²	$d\sigma/dp_t^2$ [nb/(GeV/c) ²] per Cu nucleus	$d\sigma/dp_t^2$ [nb/(GeV/c) ²] per nucleon	x_F	$d\sigma/dx_F$ (nb/Be nucleus)	$d\sigma/dx_F$ (nb/nucleon)
3.150	126±30	2.36±0.56	0.750	38±28	4.4±3.2
4.050	101±27	1.90±0.51	0.850	72±87	8.2±10.0
4.950	56±19	1.04±0.36	0.950	0±7	0.0±0.8
5.850	7±10	0.14±0.19			
6.750	14±10	0.27±0.19			
7.650	6±12	0.12±0.22			
8.550	6±9	0.11±0.17			
			p_t^2 (GeV/c) ²	$d\sigma/dp_t^2$ [nb/(GeV/c) ²] per Be nucleus	$d\sigma/dp_t^2$ [nb/(GeV/c) ²] per nucleon
			0.450	309±21	35.26±2.37
			1.350	127±13	14.45±1.51
			2.250	62±9	7.04±1.03
			3.150	17±5	1.99±0.54
			4.050	10±4	1.11±0.41
			4.950	4±3	0.47±0.36
			5.850	5±2	0.53±0.27
			6.750	0±2	0.00±0.21
			7.650	0±2	0.00±0.22
			8.550	1±2	0.08±0.21
$\cos\theta$	$d\sigma/d\cos\theta$ (nb/Cu nucleus)	$d\sigma/d\cos\theta$ (nb/nucleon)	$\cos\theta$	$d\sigma/d\cos\theta$ (nb/Be nucleus)	$d\sigma/d\cos\theta$ (nb/nucleon)
-0.90	950±461	17.8±8.6	-0.90	195±99	22.2±11.3
-0.70	1382±285	25.8±5.3	-0.70	227±49	25.9±5.6
-0.50	1226±195	22.9±3.6	-0.50	242±37	27.6±4.2
-0.30	1387±181	25.9±3.4	-0.30	249±32	28.4±3.7
-0.10	1696±185	31.7±3.5	-0.10	236±29	26.9±3.3
0.10	1601±185	29.9±3.5	0.10	287±32	32.7±3.7
0.30	1744±204	32.6±3.8	0.30	246±32	28.0±3.7
0.50	1387±209	25.9±3.9	0.50	232±37	26.4±4.2
0.70	1140±257	21.3±4.8	0.70	209±47	23.9±5.4
0.90	1041±466	19.4±8.7	0.90	186±65	21.2±7.4
ϕ (deg)	$d\sigma/d\phi$ (nb/Cu nucleus)	$d\sigma/d\phi$ (nb/nucleon)	ϕ (deg)	$d\sigma/d\phi$ (nb/Be nucleus)	$d\sigma/d\phi$ (nb/nucleon)
18.0	7.9±1.38	0.147±0.026	18.0	1.5±0.25	0.174±0.028
54.0	8.6±1.28	0.161±0.024	54.0	1.3±0.21	0.147±0.024
90.0	8.0±1.14	0.149±0.021	90.0	1.1±0.18	0.123±0.020
126.0	9.5±1.38	0.178±0.026	126.0	1.5±0.22	0.176±0.026
162.0	8.6±1.43	0.162±0.027	162.0	1.3±0.23	0.146±0.026
198.0	8.0±1.38	0.149±0.026	198.0	1.1±0.21	0.130±0.024
234.0	8.2±1.24	0.153±0.023	234.0	1.5±0.22	0.169±0.026
270.0	6.8±1.05	0.128±0.020	270.0	1.5±0.21	0.167±0.024
306.0	7.2±1.19	0.134±0.022	306.0	1.3±0.21	0.151±0.024
342.0	9.0±1.43	0.169±0.027	342.0	1.2±0.22	0.141±0.026
	(c)				
x_F	$d\sigma/dx_F$ (nb/Be nucleus)	$d\sigma/dx_F$ (nb/nucleon)			
0.050	1699±189	193.7±21.6			
0.150	1289±127	147.0±14.5			
0.250	891±90	101.7±10.3			
0.350	472±65	53.9±7.4			
0.450	242±49	27.6±5.6			
0.550	120±36	13.7±4.1			
0.650	48±31	5.5±3.5			

$$\frac{d\sigma}{dx_F} = N \int_{4M_c^2}^{4M_D^2} dM^2 \left[\frac{\hat{\sigma}_{gg}(M^2, \Lambda^2)(1-\tau)G_1(x_1)G_2(x_2)}{s(x_1+x_2)} + \frac{\hat{\sigma}_{q\bar{q}}(M^2, \Lambda^2)(1-\tau)}{s(x_1+x_2)} \sum_{k=1}^n f_k(x_1)\bar{q}_k(x_2) + \bar{f}_k(x_1)q_k(x_2) \right], \quad (1a)$$

where M is the invariant mass of the $c\bar{c}$ pair, M_c and M_D are the charm quark and D -meson masses, respectively, N is the fixed fraction of the $c\bar{c}$ production cross section leading to a particular charmonium state, $x_1(x_2)$ is the

fraction of the momentum of the beam (target) hadron which is carried by the parton:

$$x_{1,2} = 0.5 \left[\sqrt{x_F^2(1-\tau)^2 + 4\tau \pm x_F(1-\tau)} \right]. \quad (1b)$$

$\tau = M^2/s = x_1 x_2$ is the scaling variable, $G_1(x)$ and $G_2(x)$ are the gluon distribution functions, $f_k(x)$ and $q_k(x)$ are the quark distribution functions, and $\hat{\sigma}_{q\bar{q}}$ and $\hat{\sigma}_{gg}$ are the pointlike cross sections for the subprocess $q\bar{q} \rightarrow c\bar{c}$ and $gg \rightarrow c\bar{c}$ with

$$\begin{aligned} \hat{\sigma}_{gg} &= \frac{\pi\alpha_s^2}{3M^6} \left[(M^4 + 4M^2M_c^2 + M_c^4) \ln \left[\frac{M^2 + \lambda}{M^2 - \lambda} \right] \right. \\ &\quad \left. - (7M^2 + 31M_c^2) \frac{\lambda}{4} \right], \\ \hat{\sigma}_{q\bar{q}} &= \frac{8\pi\alpha_s^2}{27M^6} [M^2 + 2M_c^2] \lambda, \\ \lambda^2 &= M^4 - 4M^2M_c^2, \end{aligned} \quad (1c)$$

with α_s being the coupling constant.

ψ is either produced directly or as the decay product of the ψ' or the χ 's. We have ignored the small fraction of ψ 's that come from ψ' production and decay in the analysis that follows. However, we must allow for the relatively large fraction of ψ 's from the decays of χ states. The following expression [12] gives the $d\sigma/dx_F$ distribution of the indirectly produced ψ 's as a function of the $d\sigma/dx_F$ of the parent χ state:

$$\left. \frac{d\sigma}{dx_F} \right|_{\chi \rightarrow \psi} = \int_{\alpha_1}^{\alpha_2} \left. \frac{d\sigma}{dx_F} \right|_{\chi} \frac{M_\chi^2}{M_\chi^2 - M_\psi^2} \frac{1 - \tau_\psi}{(x_1 + x_2)_\chi} dx_F \Big|_{\chi}, \quad (2)$$

where $d\sigma/dx_F|_{\chi \rightarrow \psi}$ is the observed x_F distribution of ψ from $\chi \rightarrow \psi + \gamma$ decays, $d\sigma/dx_F|_{\chi}$ is the x_F distribution of the given χ state, M_χ and M_ψ are the masses of the χ and ψ meson, and

$$\begin{aligned} \alpha_{1,2} &= 0.5x_F|_{\psi} \frac{1 - \tau_\psi}{1 - \tau_\chi} \frac{M_\chi^2 + M_\psi^2}{M_\psi^2} \\ &\mp \frac{[(x_F)|_{\psi}^2 (1 - \tau_\psi)^2 + 4\tau_\psi]^{1/2}}{1 - \tau_\chi} \frac{M_\chi^2 - M_\psi^2}{M_\psi^2} \end{aligned}$$

with $\tau_\psi = M_\psi^2/s$ and $\tau_\chi = M_\chi^2/s$. We have assumed that in the rest frame of χ the azimuthal and $\cos\theta$ distributions of the photon are uniform (where θ is the angle between the photon direction and the beam axis). We combine this prediction of the x_F distribution of the indirectly produced ψ 's with the x_F distribution of the directly produced ψ 's to get $d\sigma/dx_F$ of the total ψ sample given by

$$\left. \frac{d\sigma}{dx_F} \right|_{\text{observed}} = (1-w) \left[\left. \frac{d\sigma}{dx_F} \right]_{\text{direct } \psi} + w \left[\left. \frac{d\sigma}{dx_F} \right]_{\chi \rightarrow \psi}, \quad (3)$$

where w is the fraction of ψ 's coming from the decay of the χ states.

The fractions of ψ 's produced via χ decay in proton-proton interactions has been measured at the CERN Intersecting Storage Rings (ISR) by experiment R806 [13] ($\sqrt{s} = 62$ GeV) to be 0.47 ± 0.08 , a similar value of

0.47 ± 0.23 was reported by Fermilab experiments E673 [14] ($\sqrt{s} = 18.9$ GeV) in $p\text{Be}$ interactions and more recently a value of 0.30 ± 0.04 has been reported by experiment E705 [15] for $p\text{Li}$ ($\sqrt{s} = 23.76$ GeV). No measurement has been reported for ψ 's produced in $\bar{p}N$ interactions at 125 GeV/c. Although the value of $w = 0.47$ (from the data closest in energy to ours, $\sqrt{s} = 15.36$ GeV) was adopted for the purposes of the analysis in this paper, varying the value of w from 0.30 to 0.47 (a range that includes all the measured ratios in proton interactions quoted above and those for π^- interactions quoted in Sec. VII below) changes the extracted structure function parameters by less than 2%. The x_F distribution of the indirectly produced ψ 's is also found to be insensitive to the p_t distribution of the parent χ or to the angular distribution of the photon in the $\chi \rightarrow \psi + \gamma$ decay.

The Duke and Owens (DO) set 1 quark structure functions for the nucleon [16] describes well our Drell-Yan data [6] for $\langle Q^2 \rangle = 25$ (GeV/c²)². We have used these structure functions with the SLDM and find that the Q^2 dependence of the structure function within our limits of integration $4M_c^2 < M^2 < 4M_D^2$ is not strong. Therefore, we fix $Q^2 = M_{cc}^2$ and ignore the evolution of the structure functions with Q^2 . The choice of the value of the parameter Λ ($= 0.2$ GeV/c²) and the mass of the charmed quark ($= 1.5$ GeV/c²) affect only the overall normalization and not the shape of the $d\sigma/dx_F$ spectra.

We have fitted the x_F distribution of the ψ 's from our $\bar{p}W$ data using the SLDM prediction [Eqs. (1) and (3)] with the DO set 1 quark and gluon structure functions determined at $Q^2 = M_\psi^2$ leaving the overall normalization N free. A value of $N = 0.188 \pm 0.002$ is found. Figure 3 shows the excellent agreement (χ^2 per degree of freedom equal 1.0) between the fit and the data. From the results of this fit we estimate that 48% of ψ 's are produced through gluon-gluon fusion.

We can also write the prediction of the SLDM for the

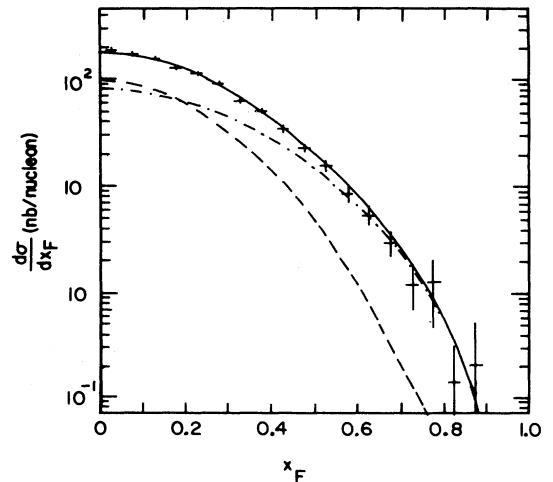


FIG. 3. $d\sigma/dx_F$ for ψ production by 125 GeV/c $\bar{p}W$ interactions. The solid line is the SLDM prediction using DO set 1 structure functions and keeping the overall normalization as a free parameter. The dashed and the dot-dashed line are the gg and the $q\bar{q}$ contributions, respectively.

TABLE III. Cross-section ratio for ψ production by \bar{p} 's and p 's on nuclear targets at different energies. We have used the Lyons [18] parametrization for pN interactions as a function of $\sqrt{\tau}$ to estimate the cross section for ψ production by protons at the E537 energy of $\sqrt{s} = 15.3$ GeV.

Experiment	Beam momentum (GeV/c)	\sqrt{s} (GeV/c ²)	$R(\sqrt{s}; \bar{p}/p)$
Ω (Ref. [17])	39.5	8.6	5.26 ± 0.83
E537	125.0	15.3	2.0 ± 0.3
NA3 (Ref. [8])	150.0	16.8	2.35 ± 0.3
NA3 (Ref. [8])	200.0	19.4	1.46 ± 0.25

ratio of the \bar{p} -nucleon to p -nucleon total ψ production cross sections at a particular \sqrt{s} as

$$R_{\text{SLDM}}(\sqrt{s}; \bar{p}/p) = \frac{[\sigma_{q\bar{q}}^{\bar{p}}(\sqrt{s}) + \sigma_{gg}^{\bar{p}}(\sqrt{s})]}{[\sigma_{q\bar{q}}^p(\sqrt{s}) + \sigma_{gg}^p(\sqrt{s})]},$$

where $\sigma_{q\bar{q}}^h(\sigma_{gg}^h)$ is the integral over x_F of the $q\bar{q}$ (gg) part of Eq. (1), and h denotes the beam hadron. The dependence of the ψ production cross section on the atomic number is similar for \bar{p} and π^- beams [4]. Providing the same is true for proton-nucleus interactions, then the ratio R should be approximately independent of the specific target nucleus. In Table III, we list measured cross-section ratios $R(\sqrt{s}; \bar{p}/p)$ for ψ production with antiproton and proton beams on nuclear targets.

We have checked the possibility that there may be a relative normalization of the $q\bar{q}$ and gg processes (beyond the expectation of the SLDM) by fitting the variation of the ratio R as a function of \sqrt{s} with two different normalization factors, $N_{q\bar{q}}$ and N_{gg} :

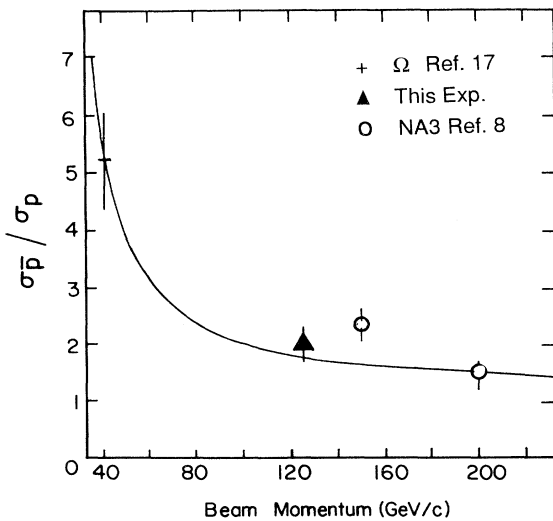


FIG. 4. Comparison of the ratios of inclusive ψ production cross sections from $\bar{p}N$ and pN interactions (Table III) with the prediction of the SLDM using DO set 1 structure functions.

$$R_{\text{SLDM}}(\sqrt{s}; \bar{p}/p) = \frac{\sigma_{q\bar{q}}^{\bar{p}}(\sqrt{s}) + K \sigma_{gg}(\sqrt{s})}{\sigma_{q\bar{q}}^p(\sqrt{s}) + K \sigma_{gg}(\sqrt{s})}$$

with $K = \frac{N_{gg}}{N_{q\bar{q}}}$. (4)

Fitting the ratio of Eq. (4) to the data of Table III and using the DO set 1 structure functions for quarks and gluons, we obtain a value of $K = 1.08 \pm 0.3$. Therefore, we have fixed $K = 1.0$ for the remainder of the analysis. In Fig. 4, we compare the measured values of $R(\sqrt{s}; \bar{p}/p)$, from Table III, with the R_{SLDM} prediction ($K = 1.0$) showing very good agreement.

VI. ANTIPROTON GLUON STRUCTURE FUNCTION

Although the DO set 1 gluon structure function agrees well with our $\bar{p}W$ data, we investigated a simpler form for the gluon structure functions. We use as inputs the valence and sea quark structure functions given by DO set 1 and parametrize the gluon structure functions of the beam antiproton and the target nucleons in the form

$$xG(x) = \beta(1-x)^\alpha(1+\gamma x). \quad (5)$$

The parameters α, β, γ , and the overall normalization N of the SLDM are determined from this fit. Although the parameters N and β have different physical origins, they are correlated since both contribute to the overall normalization.

The parameter β can be expressed as a function of the other parameters of Eq. (5) using the momentum sum rule as an extra constraint. Our choice of the valence and sea quark structure functions implies that 52% of the nucleon momentum is carried by the quarks. Therefore, to conserve momentum the gluon structure function must satisfy

$$\int_0^1 xG(x)dx = 0.48. \quad (6)$$

Because we do not measure ψ production over the entire x range of the integral, Eq. (6), but only for

TABLE IV. Extracted gluon structure function parameters from the fit E537- \bar{p} , including the fraction of momentum carried by gluons overall ($0.0 < x < 1.0$), that for ($0.038 < x < 1.0$) and the fraction of ψ produced by gluon fusion. Also shown is the DO set 1 results for comparison. (Note that the uncertainty due to the scaling of the cross sections to nb/nucleon is 3.1%.)

Parameter	E537- \bar{p}	Duke and Owens set 1
χ^2/N_{DF}	1.0	1.0
N	0.188 (fixed)	0.188 ± 0.002
α	6.83 ± 0.5	
β	2.15 ± 0.7	
$\gamma \int_0^1 xG(x)dx$	5.85 ± 0.95	
$\int_0^1 xG(x)dx$	$46\% \pm 3\%$	48%
$\int_{0.038}^1 xG(x)dx$	$38\% \pm 2.5\%$	38%
$\sigma_{gg}/(\sigma_{gg} + \sigma_{q\bar{q}})$	$48\% \pm 3\%$	48%

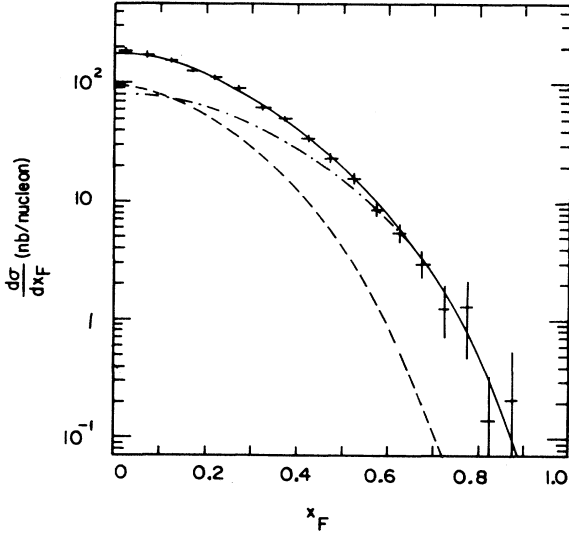


FIG. 5. $d\sigma/dx_F$ for ψ production by 125 GeV/c $\bar{p}W$ interactions. The solid line represents the best fit of the parametrization of the gluon structure function $xG(x)=\beta(1-x)^\alpha(1+\gamma x)$. The dashed and the dot-dashed line are the gg and the $q\bar{q}$ contributions, respectively.

$0.038 \leq x \leq 1.0$, we have assumed that the gluon structure function parametrization is valid for all regions of x in order to apply the constraint of Eq. (6). Rather than determining β *a priori*, we constrain the overall normalization N and determine all the gluon structure function parameters. In this way, the degree to which Eq. (6) is satisfied by the fitted $G(x)$ can be used as a criterion for deciding on the correctness of the extracted structure function. Table IV shows the results of the fit to the $\bar{p}W$ data, E537- \bar{p} , including the integrated gluon momentum fraction for the entire x region ($0.0 < x < 1.0$), for the region of sensitivity of the experiment ($0.038 < x < 1.0$) and the fraction of ψ 's produced through gluon fusion.

The results of the fit E537- \bar{p} are in good agreement with the DO set 1 gluon structure functions, and give a reasonable value for the integrated gluon fraction. Figure 5 shows the results of the fit to the differential cross section $d\sigma/dx_F$ for our $\bar{p}W$ data.

The effects of heavy nuclear targets are most important at high x_F [4]. To check for the sensitivity to these effects, we have extracted the gluon structure function from the $\bar{p}W$ data at $x_F \leq 0.5$ using our parametrization. The values of the parameters of the gluon distributions obtained using this limited x_F region are consistent within statistical errors with those obtained using the entire range of x_F .

Our results for the parametrization for the \bar{p} gluon structure is

$$xG(x) = (2.15 \pm 0.7)[1-x]^{(6.83 \pm 0.5)}[1 + (5.85 \pm 0.95)x] .$$

VII. π^- GLUON STRUCTURE FUNCTION

The π^- quark structure functions are not as well determined as the nucleon quark structure functions and, since

a larger percentage of ψ 's produced in π^- collisions are in the high x_F region, we expect stronger nuclear target effects [4].

The fraction of ψ 's produced via χ decay in π^- nucleon interactions has been measured by experiment WA11 [10] ($\sqrt{s} = 18.6$ GeV) to be 0.305 ($0.177 \pm 0.035 \pm 0.015$ from χ^1 and $0.128 \pm 0.023 \pm 0.15$ from χ^2 decays), by experiment E673 [14] ($\sqrt{s} = 18.9$ GeV) as 0.31 (0.2 ± 0.08 from χ^1 and 0.11 ± 0.06 from χ^2 decays) and more recently experiment E705 [15] published a value of 0.37 ± 0.03 for π^-Li at 300 GeV/c.

For our extraction of the gluon structure functions of the π^- , we have used the WA11 [10] ($\sqrt{s} = 18.9$ GeV) measurements to set the fraction of ψ 's coming from χ 's for our π^-N data ($\sqrt{s} = 15.3$ GeV), the target nucleon DO set 1 gluon, valence and sea quark structure functions (as they describe well our $\bar{p}W$ data), the NA3 [8] determination of the sea quark pion structure function as $0.238(1-x)^{8.7}$ which predicts that 15% of the total momentum is carried by the sea quarks, and the π^- valence quark structure functions determined from our own measurements of Drell-Yan production of high-mass muon pairs [6,19,20].

The parametrization of Ref. [6(b)] for the valence quark structure function of π^- :

$$xV(x) = Ax^a(1-x)^b \quad (7)$$

has been scaled to $Q^2 = M_\psi^2$ using the method of Altarelli-Parisi [21] to obtain the values of A , a , and b given in Table V. Also shown for comparison in the Table is the NA3 [8] valence quark structure function. Different E537 π^- fits corresponding to different normalization constraints to our Drell-Yan data [6,20] have little effect on the overall result.

With this choice for the quark structure function, we parametrize the gluon distribution of π^- as

$$xG(x) = \beta(1-x)^\alpha . \quad (8)$$

We have fitted both our π^-W and π^-Be data using the quark distributions of Table V as input to the SLDM, leaving the overall normalization and the exponent α free to vary. The results for W and Be targets are shown in Table VI, the fraction of momentum carried by the gluons [$\beta/(\alpha+1)$] has been fixed for the fit as shown. In addition, the calculated fraction of the ψ produced via gluon fusion in π^-W and π^-Be interactions is also shown.

The resulting value of the overall normalization constant is in agreement with that obtained using the SLDM with our \bar{p} data. Although the extracted gluon structure functions are not sensitive to the choice of the quark

TABLE V. Valence quark structure function parameters of Refs. [6,19,20] evolved to $Q^2 = M_\psi^2$ and of Ref. [8] used in extracting the gluon structure function of the π^- .

Set	A	a	b	$\int_0^1 xV(x)dx$ (%)
E537- π^-	0.681	0.454	1.125	35
NA3 (Ref. [8])	0.52	0.40	0.78	36

TABLE VI. The parameters of the π^- gluon structure function obtained by fitting with the input valence quark distribution, $V(x)$, for the W and Be data. The fraction of ψ produced via gluon fusion obtained from the fit is also shown. Note that the error due to the scaling of the cross section to nb/nucleon is an additional 3.1%.

$V(x)$	$\beta/\alpha+1$ (fixed) (%)	$\alpha(W)$	$\alpha(Be)$	$N(W)$	$N(Be)$	$\sigma_{gg}/\sigma_{\pi^-}(W)$ (%)	$\sigma_{gg}/\sigma_{\pi^-}(Be)$ (%)
E537- π^-	50	1.98 ± 0.06	1.2 ± 0.2	0.187 ± 0.002	0.17 ± 0.004	74 ± 2	76 ± 8
Na3 (Ref. [8])	49	2.03 ± 0.06	1.3 ± 0.2	0.193 ± 0.002	0.17 ± 0.004	73 ± 3	75 ± 7

structure function set, as seen in Table VI they depend strongly on the particular target nucleus used. In Fig. 6, we present our data for W, and in Fig. 7 for Be, and the predictions of the SLDM model using the E-537- π^- pion valence quark structure function. The solid line represents the prediction for the gluon structure function extracted from the Be data. In Fig. 7, we include the gluon structure function based on the fit to the W data to show the strength of the A dependence.

As in the case of determining the \bar{p} gluon structure function we use the ratios of the ψ production cross sections to check the validity of the fits. The ratios of the production cross sections for $pN \rightarrow \psi + X$ to $\pi^- N \rightarrow \psi + X$,

$$R(\sqrt{s}; p/\pi^-) = \frac{\sigma(pN \rightarrow \psi + X)}{\sigma(\pi^- N \rightarrow \psi + X)},$$

are sensitive only to the integral of the parton distribution functions. In Table VII we summarize the measured ratios as function of beam energy from several experiments.

The gluon structure functions extracted from the Be and the W data have been used to predict the ratio of the total cross section σ_p/σ_{π^-} as a function of beam momen-

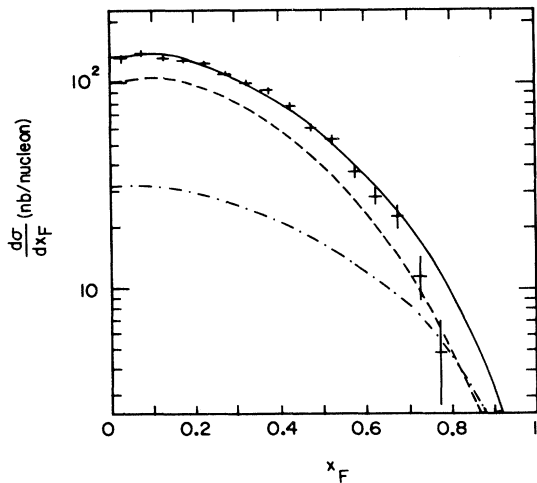


FIG. 6. Best fit (solid line) using the E537- π^- quark structure functions to the $d\sigma/dx_F$ distribution for ψ production in 125 GeV/c π^- -W interactions. The dashed and the dot-dashed line are the gg and the $q\bar{q}$ contributions, respectively.

tum. This prediction is compared in Fig. 8 to the data in Table VII. The momentum dependence of the ratio σ_p/σ_{π^-} is described satisfactorily by both sets of structure functions.

For comparison, experiment NA3 [8] has extracted the gluon structure function of π from the “hard component” of ψ production in π^- -Pt interactions using an analysis with significantly different assumptions about the production model for the ψ 's:

$$xG(x) \sim (1-x)^{2.38 \pm 0.06 \pm 0.1}.$$

WA11 [10] using a Be target has extracted a gluon structure function

$$xG(x) \sim (1-x)^{1.9 \pm 0.3}.$$

Our best estimation of the π^- gluon structure function from experiment E537 is

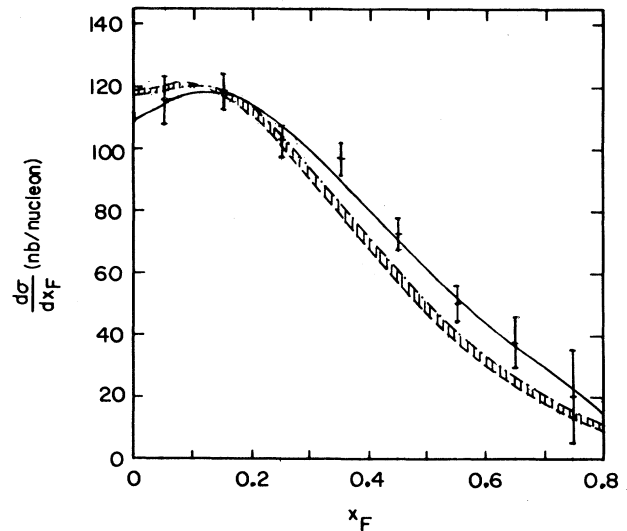


FIG. 7. $d\sigma/dx_F$ for ψ production in 125 GeV/c π^- -Be interactions. The solid line is the best fit using E537- π^- quark structure functions. The band shows the range of predictions from the SLDM varying the π^- gluon structure function parameters extracted from the W data by \pm one standard deviation from the best fit. The difference in structure functions extracted from Be and W targets is manifest.

TABLE VII. Cross-section ratios for ψ production by p and π^- beams on nuclear targets measured at different energies. To obtain the ratio for this experiment we have used the Lyons [18] parametrization to estimate the cross section for ψ production by protons at 125 GeV/c.

Experiment	Beam momentum (GeV/c)	\sqrt{s} (GeV/c ²)	$\sigma_p/\sigma_{\pi^-}=R(\sqrt{s};p/\pi^-)$
Ω (Ref. [17])	39.5	8.6	0.17±0.02
E537	125.0	15.3	0.45±0.05
NA3 (Ref. [8])	150.0	16.8	0.42±0.04
NA3 (Ref. [8])	200.0	19.4	0.53±0.05

$$xG(x) = (1.49 \pm 0.03)[1-x]^{(1.98 \pm 0.06)}$$

from the π^-W data

and

$$xG(x) = (1.10 \pm 0.10)[1-x]^{(1.20 \pm 0.20)}$$

from the π^-Be data .

VIII. TRANSVERSE MOMENTUM OF ψ

In Figs. 9(a) and 9(b), we present the $d\sigma/dp_t^2$ spectra for $\bar{p}W$ and π^-W . The experimental data is well described by the empirical form

$$(1 + p_t^2/\alpha^2)^\beta \quad (9)$$

with $\alpha = 2.79 \pm 0.2$, $\beta = -8.03 \pm 0.96$ for the $\bar{p}W$ data and $\alpha = 2.67 \pm 0.12$, $\beta = -6.87 \pm 0.5$ for the π^-W data.

In Figs. 10(a) and 10(b), we show the variation of $\langle p_t \rangle$ as a function of x_F . In an earlier publication [6], it was

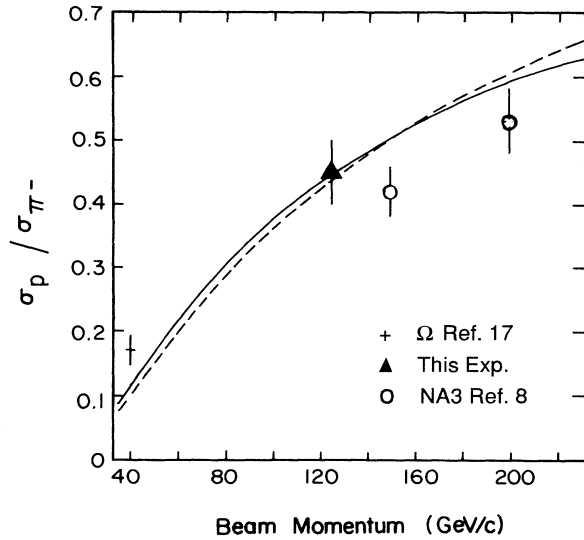


FIG. 8. Comparison of the ratios of the inclusive ψ production cross sections from p and π^- of Table VII with the predictions of the SLDM using the E537- π^- quark structure functions and the gluon structure function extracted from this experiment's Be data (solid line) and W data (dashed line).

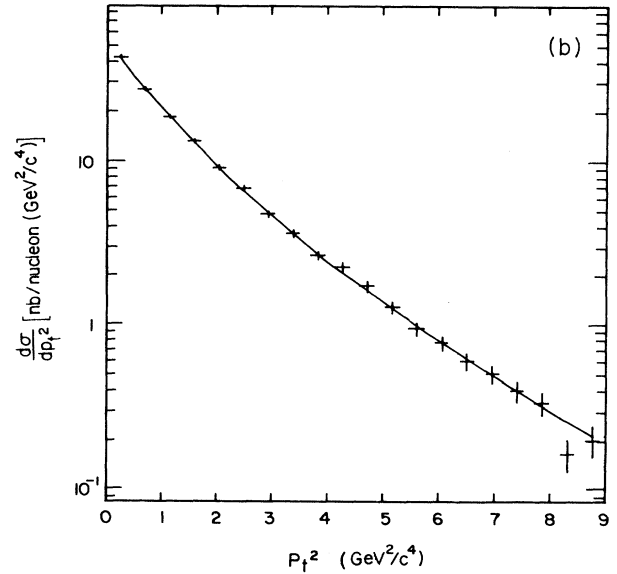
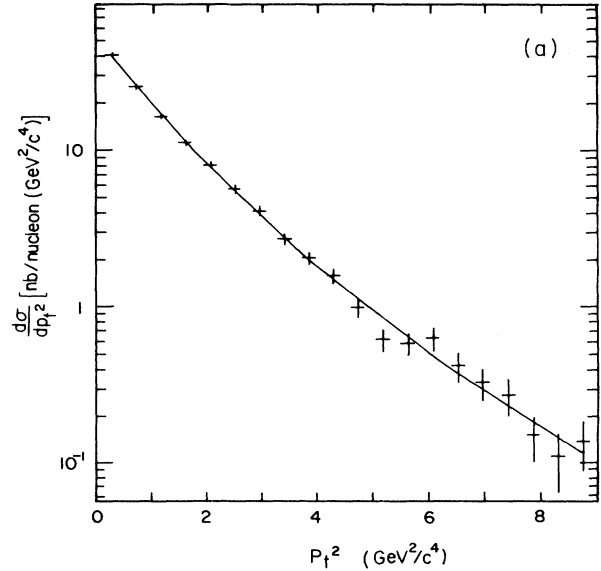


FIG. 9. (a) $d\sigma/dp_t^2$ vs p_t^2 for ψ production in 125 GeV/c $\bar{p}W$ interactions. The solid line is an empirical fit. (b) $d\sigma/dp_t^2$ vs p_t^2 for ψ production in 125 GeV/c π^-W interactions. The solid line is an empirical fit.

shown that nuclear effects distort the shape of the p_t distribution independently of the x_F region examined. Therefore, the systematic decrease of the mean p_t vs x_F appears not to be caused by heavy nucleus effects.

IX. ANGULAR DISTRIBUTIONS

Finally, we have studied the angular distributions of the ψ 's to gain additional information about the ψ production mechanism [22]. We show the Gottfried-Jackson [23] frame angular distributions in θ , the angle of the positive muon with respect to the beam in the rest frame of ψ . Figures 11(a) and 11(b) show that the angular distributions are essentially flat. Fitting the angular distributions to the form

$$d\sigma/d\cos\theta \propto 1 + \lambda\cos^2\theta,$$

we obtain $\lambda = -0.115 \pm 0.061$ for \bar{p} 's and $\lambda = 0.028 \pm 0.004$ for π^- 's. Similarly, the azimuthal angle ϕ distribution is flat within errors. The isotropic

behavior of the data is independent of the x_F and p_t regions in both \bar{p} and π^- interactions as shown in Figs. 12 and 13.

We have also studied the A dependence of the ψ production cross sections as a function of $\cos\theta$ and ϕ by forming the ratios

$$r_1(\cos\theta; W/\text{Be}) = \frac{1/A_W [d\sigma/d\cos\theta]_W}{1/A_{\text{Be}} [d\sigma/d\cos\theta]_{\text{Be}}}$$

and

$$r_2(\phi; W/\text{Be}) = \frac{1/A_W [d\sigma/d\phi]_W}{1/A_{\text{Be}} [d\sigma/d\phi]_{\text{Be}}}.$$

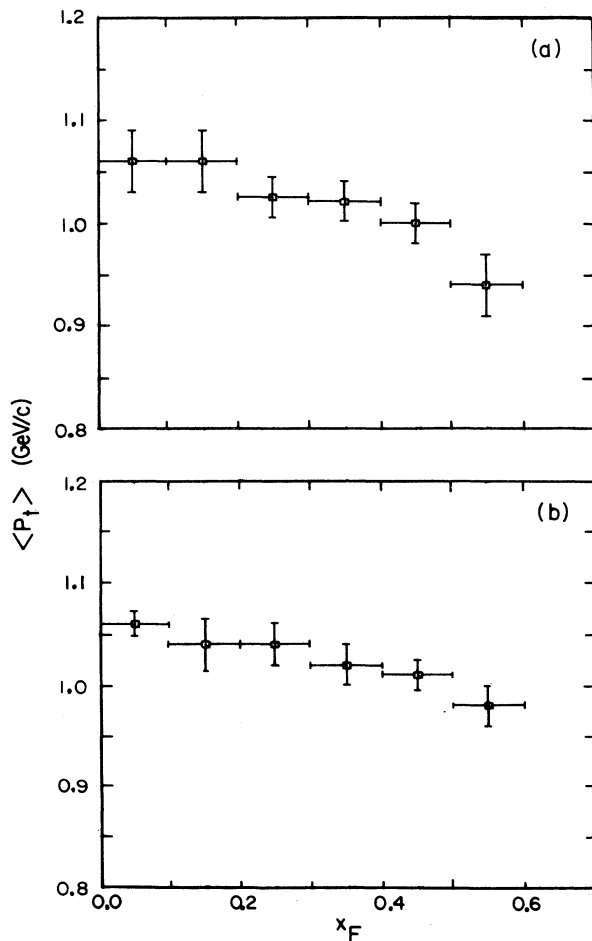


FIG. 10. $\langle p_t \rangle$ vs x_F for ψ production in 125 GeV/c interactions, (a) $\bar{p}W$ and (b) π^-W data.

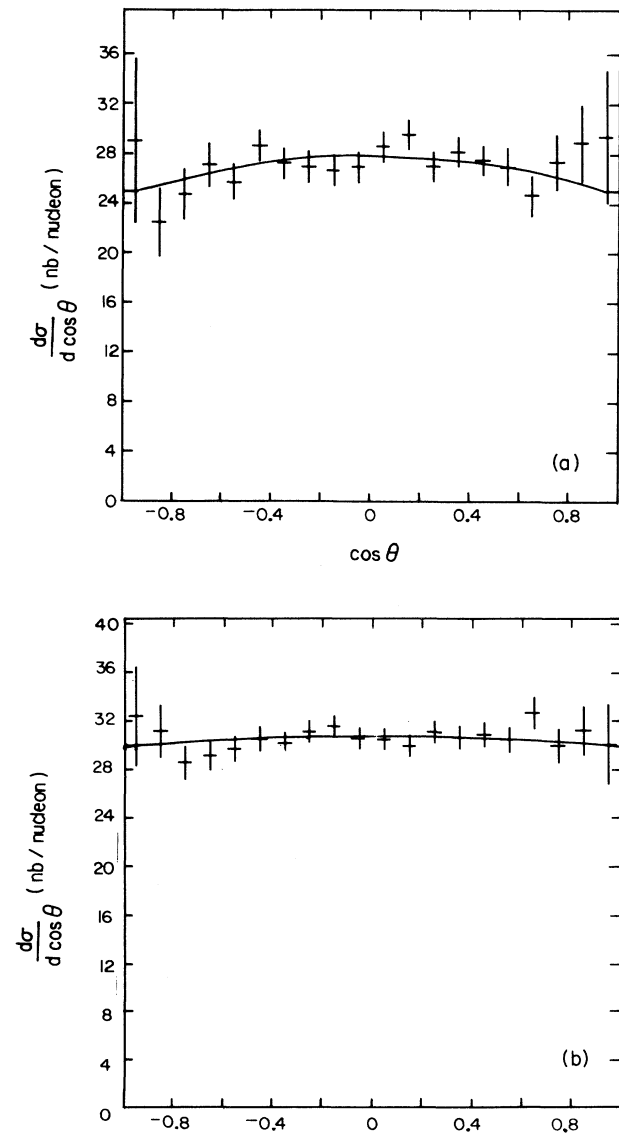


FIG. 11. Gottfried-Jackson $\cos\theta$ distributions for ψ decay from 125 GeV/c interactions, (a) $\bar{p}W$ and (b) π^-W data.

Both ratios r_1 and r_2 are flat within statistical errors as a function of $\cos\theta$ and ϕ for both the \bar{p} and π^- data. The average value of the ratios, 0.73 ± 0.04 for the \bar{p} data and 0.70 ± 0.02 for the π^- data, are consistent with an overall suppression of ψ production in the heavy targets. If one parametrizes the A dependence in the form $\sigma \sim A^\alpha$, these ratios give $\alpha = 0.90 \pm 0.05$ and 0.88 ± 0.03 , respectively.

X. CONCLUSIONS

We have studied ψ hadronic production in $\bar{p}N$ and π^-N interactions at 125 GeV/c. We have measured the total cross section for the production of ψ and ψ' , the differential cross section $d\sigma/dx_F$ for both \bar{p} and π^- beams with Be, Cu, and W targets and determined the gluon structure functions of the \bar{p} 's and π^- 's by fitting the x_F distributions. For the antiproton we find a parametrization which is in good agreement with our $\bar{p}W$ data and the Duke and Owens (set 1) structure functions:

$$xG(x)_{\bar{p}} = (2.15 \pm 0.7)[1-x]^{(6.83 \pm 0.5)}[1 + (5.85 \pm 0.95)x].$$

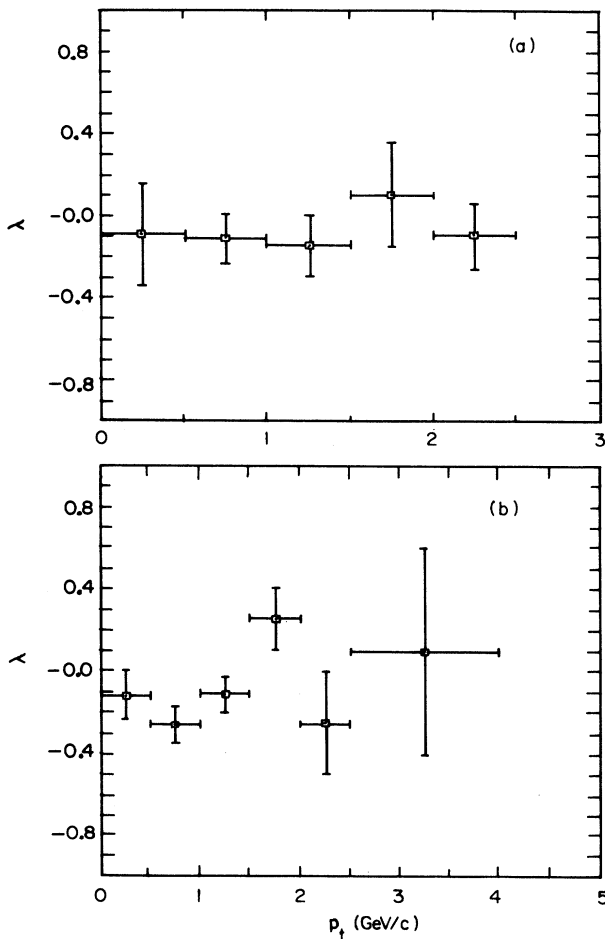


FIG. 12. λ , the coefficient in the $(1-\lambda \cos^2\theta)$ fit to the Gottfried-Jackson decay angle of ψ 's, as a function of p_t and integrated over all x_F for 125 GeV/c interactions, (a) $\bar{p}W$ data and (b) π^-W data.

Nuclear target effects significantly change the shape of the observed x_F distributions in our π^- data. Our data were sufficient to give statistically different results for the π^- gluon structure functions extracted separately from the π^-W and π^-Be data:

$$xG(x)_{\pi^-} = (1.49 \pm 0.03)[1-x]^{(1.98 \pm 0.06)}$$

from π^-W production

and

$$xG(x)_{\pi^-} = (1.10 \pm 0.10)[1-x]^{(1.20 \pm 0.20)}$$

from π^-Be production.

We have also measured the transverse momentum and decay angular distributions of the ψ 's. Isotropic angular distributions are observed.

ACKNOWLEDGMENTS

We thank the staff of Fermilab for their support in the construction and operation of the experiment. This work was performed at Fermilab and supported by the U.S.

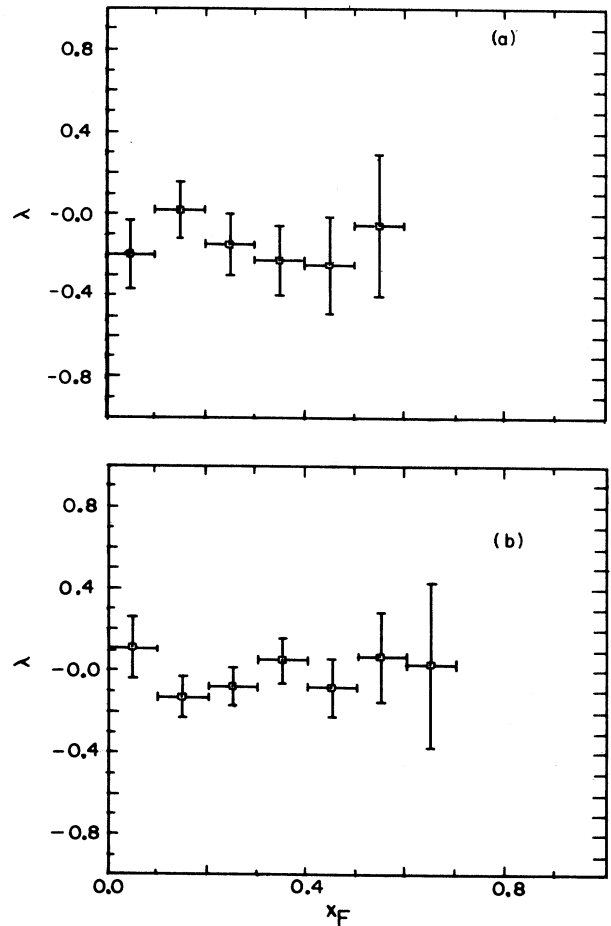


FIG. 13. λ , the coefficient in the $(1-\lambda \cos^2\theta)$ fit to the Gottfried-Jackson decay angle of ψ 's, as a function of x_F and integrated over all p_t for 125 GeV/c interactions, (a) $\bar{p}W$ data and (b) π^-W data.

Department of Energy (Contract No. DE-AC02-76CHO3000), The North Atlantic Treaty Organization Scientific Affairs Division, the International Programs and High Energy Physics Divisions of the National Sci-

ence Foundation, the Natural Sciences and Engineering Research Council of Canada, the Quebec Department of Education, and the Hellenic Science and Technology Agency.

-
- [1] See, for example, R. Baier and R. Rückl, *Z. Phys. C* **19**, 251 (1983).
- [2] J. J. Aubert *et al.*, *Nucl. Phys.* **B293**, 740 (1987).
- [3] J. J. Aubert *et al.*, *Nucl. Phys.* **B272**, 158 (1986).
- [4] S. Katsanevas *et al.*, *Phys. Rev. Lett.* **60**, 2121 (1988).
- [5] E. Anassontzis *et al.*, *Nucl. Instrum. Methods A* **242**, 215 (1986).
- [6] (a) E. Anassontzis *et al.*, *Phys. Rev. Lett.* **54**, 2572 (1985);
(b) E. Anassontzis *et al.*, *Phys. Rev. D* **38**, 1377 (1988).
- [7] H. Areti *et al.*, *Nucl. Instrum. Methods* **212**, 135 (1983).
- [8] J. Badier *et al.*, *Z. Phys. C* **20**, 101 (1983).
- [9] Particle Data Group, G. P. Yost *et al.*, *Phys. Lett. B* **204**, 1 (1988).
- [10] Y. Lemoigne *et al.*, *Phys. Lett.* **113B**, 509 (1982); J. G. McEwen *et al.*, *ibid.* **121B**, 198 (1983).
- [11] M. Glück *et al.*, *Phys. Rev. D* **17**, 2324 (1978); M. Glück and E. Reya, *Phys. Lett.* **79B**, 453 (1978); V. Barger *et al.*, *Z. Phys. C* **6**, 169 (1980); V. Barger *et al.*, *Phys. Lett.* **91B**, 253 (1980); P. Chiappetta and P. Mery, *Phys. Rev. D* **32**, 2337 (1985).
- [12] G. Voulgaris, Ph.D. thesis, University of Athens, 1984; S. Tzamarias, Ph.D. thesis, University of Athens, 1986.
- [13] C. Kourkoumelis *et al.*, *Phys. Lett.* **81B**, 405 (1979).
- [14] D. A. Bauer *et al.*, *Phys. Rev. Lett.* **54**, 753 (1985).
- [15] L. Antoniazzi *et al.*, *Phys. Rev. Lett.* **70**, 383 (1993).
- [16] D. W. Duke and J. F. Owens, *Phys. Rev. D* **30**, 49 (1984).
- [17] M. J. Corden *et al.*, *Phys. Lett.* **96B**, 411 (1980).
- [18] L. Lyons, *Prog. Part. Nucl. Phys.* **7**, 169 (1981).
- [19] S. Katsanevas, Ph.D. thesis, University of Athens, 1982.
- [20] W. Schappert, Ph.D. thesis, McGill University, 1984.
- [21] G. Altarelli and G. Parisi, *Nucl. Phys.* **B126**, 298 (1977).
- [22] B. L. Ioffe, *Phys. Rev. Lett.* **39**, 1589 (1977); J. Cleymans *et al.*, *Phys. Lett.* **106B**, 143 (1981); J. H. Kühn, *ibid.* **89B**, 385 (1980).
- [23] K. Gottfried and J. D. Jackson, *Nuovo Cimento* **33**, 309 (1964).